



RESEARCH ARTICLE

Comparison of Computed Tomographic Images of Hepatic VX2 Carcinoma Experimentally Induced in Different Methods: Correlated with Histopathologic Features

YI Kim, JW Chung, YK Choi¹ and KC Lee^{2*}

Department of Radiology, Seoul National University College of Medicine, Seoul 110-744; ¹College of Veterinary Medicine, Konkuk University, Seoul 143-751; ²Veterinary Clinical Science, College of Veterinary Medicine, Chonbuk National University, Jeonju 561-756, Republic of Korea

*Corresponding author: kclee@jbnu.ac.kr

ARTICLE HISTORY

Received: December 27, 2012
Revised: June 17, 2013
Accepted: August 07, 2013

Key words:

Computed tomography
Liver
Metastatic tumor model
Rabbit
VX2 carcinoma

ABSTRACT

To compare characteristics of computed tomographic images of hepatic tumors induced by intra-mesenteric venous and intraparenchymal injection of VX2 carcinoma in rabbits. Thirty two New Zealand White rabbit were divided into two groups; group I for metastatic tumor model (n=8) by injection of 0.1 ml tumor homogenate into mesenteric vein, and group II for solitary tumor model (n=24) by direct intraparenchymal injection of 1 mm tumor cubes. Dual-phase computed tomography (CT) was performed on day 10, 17, and 24 post-tumor implantation. On day of each CT follow-up, 2 or 3 rabbits in both groups were sacrificed for histopathologic examinations which were correlated with CT findings. Tumor creation rates were 100% in Group I, and 87.5% in Group II. In group I, arterial phase showed multiple tiny lesions on day 10, and hypodense lesions with peripheral rim enhancement and central hyperdensity (target appearance) on day 17 and 24 post-implantation. Target appearance of group I was more distinctive on portal phase, and was correlated with the viable tumor tissue core surrounded by cystic spaces in histopathologic findings. In group II, arterial phase revealed ill-defined hypodense lesions with peripheral rim enhancement during entire follow-up periods, and rim enhancement was disappeared on portal phase. Viable tumor cells in group II were mainly found in periphery of tumor with apparent central necrosis, and these observations were well correlated with CT findings. This study showed specific characteristics corresponding to each implantation method, and will provide beneficial information for experimental studies using hepatic VX2 carcinoma.

©2013 PVJ. All rights reserved

To Cite This Article: Kim YI, JW Chung, YK Choi and KC Lee, 2014. Comparison of computed tomographic images of hepatic VX2 carcinoma experimentally induced in different methods: correlated with histopathologic features. Pak Vet J, 34(1): 120-123.

INTRODUCTION

Screening for primary or metastatic hepatic cancer has been paid much attention to for the last several decades (Wolf *et al.*, 1990). To test novel diagnostic modalities or therapeutic interventions, well-established hepatic tumor models are essential. Since the splanchnic anatomy of the rabbit is similar to humans and well reported (Seo *et al.*, 2001), many hepatic tumor models have been developed and studied in rabbits using VX2 carcinoma (Shope and Hurst, 1993; Luo *et al.*, 2010; Sonoda *et al.*, 2012). Several tumor induction methods have been introduced previously. In the solitary hepatic tumor model, a tumor cell suspension or a dry tumor fragment is directly injected onto the hepatic

parenchyma after laparotomy (Koishi *et al.*, 1994; Schneider *et al.*, 1997), or under ultrasonography-guidance (Lee *et al.*, 2008). In the metastatic tumor model, a tumor cell suspension is injected into the portal venous system (Gnant *et al.*, 1999). Tumor implantation methods have been selected mainly by the researcher's preference, but the imaging features of the hepatic tumors induced by each different method have not been fully investigated yet. In this study, we created two different hepatic tumor models by intra-portal venous and intra-hepatic parenchymal injection of VX2 carcinoma in rabbits, and analyzed serial CT findings of tumors which were correlated with histopathologic features with attention to the differences between both implantation methods.

MATERIALS AND METHODS

Animals: Thirty-two adult male New Zealand white rabbits, weighing 2.5 to 3.2 kg were used in this study. The experiment was designed in accordance with the Guide for the Care and Use of Laboratory Animals, and approved by Animal Use and Care Committee of Chonbuk National University. The animals were anaesthetized with an intramuscular injection of a mixture consisting of ketamine hydrochloride (Ketalar, Yuhan Yanghang, Seoul, Korea) and xylazine hydrochloride (Rumpun, Bayer Korea, Seoul, Korea) for all experimental procedures.

Groups by tumor implantation method: The animals were divided into two groups according to tumor implantation methods; group I for metastatic tumor model ($n=8$), and group II for solitary tumor model ($n=24$).

Metastatic tumor model (Group I): Tumor implantation was performed as described previously with modification (Kapanen *et al.*, 2003). We selected the mesenteric vein for portal approach, because the mesenteric vein is directly connected to the main portal vein, and the procedure is easier and less invasive than direct portal vein injection. After laparotomy, the mesenteric vein was cannulated using a 20-gauge intravenous cannula, and 0.1 ml tumor tissue suspension was injected and flushed with saline. The mesenteric vein was ligated at both the proximal and distal end of the puncture site to control bleeding.

Solitary tumor model (Group II): After laparotomy the left hepatic lobe was exposed, and tumor fragments (1x1 mm) were inoculated onto the left lobe using an 18-gauge Seldinger needle. The puncture site was gently compressed by a cotton gauze to prevent bleeding and extravasation for 60 seconds. The wound was then closed in a routine manner.

Radiologic examination: Spiral CT machine (MX 8000, Philips medical system, DA best, Netherlands) was performed on day 10, 17 and 24 post-tumor implantation. After a coronal scout view, a non-enhanced scan was performed through the liver at 120 Kv, 200 mA, with a section thickness of 3 mm, a pitch of 1, and a FOV of 13 x 13 cm, 512 x 512 matrix. The intravenous contrast material used was iopromide (Ultravist 370, Schering, Berlin, Germany). An 8 ml of contrast agent was injected at a rate of 0.3 ml/sec using a mechanical power injector. A contrast enhanced CT of the liver was then performed with 1 mm collimation and a pitch of 1 during the hepatic arterial phase (15 seconds after the injection) and the portal venous phase (4 seconds after the end of the arterial phase). Two radiologists (JWJ, KRS) evaluated CT findings such as the size and number of visually distinguishable nodules of the hepatic tumor, as well as their enhancement pattern in the arterial and portal phase using a picture archive and communication system (Maroview, Marotech, Seoul, Korea). The two radiologists reached a consensus for each evaluation after discussion.

Pathologic examination: Two or three rabbits were sacrificed immediately after CT scanning at each follow-up day. The abdominal cavity and solid organs were inspected

for the presence of a tumor. Photographs of the liver and abdominal cavity were taken. The liver was then fixed in 10% formalin, and subsequently cut into serial 3-mm axial sections matching to the CT plane for evaluating the tumor number, size, and growth pattern, which were recorded for correlation with CT findings. Representative tissue slices were embedded in paraffin for further microsection and subsequent staining with hematoxylin and eosin. A pathologist (YKC) together with one radiologist (JWJ) assessed histopathological findings that might correspond to the CT features of the tumor and the adjacent liver parenchyma.

RESULTS

Radiologic findings

Group I (metastatic tumor model): All rabbits (100%) had numerous tumor nodules in the entire liver lobes. Most lesions had hyperattenuating central spots which made the tumor look like ‘target’. On arterial phase, several tiny enhancing spots at day 10 (Fig. 1A) and multiple ill-defined peripheral enhancing lesions scattering in the liver at day 17, (Fig. 1C) were observed. Those lesions became hypodense in portal phase (Fig. 1D). The target appearance was more distinctive at and tumor sizes and numbers were increased, day 24 (Fig. 1E, F). Tumors were too small to measure their sizes at day 10 post-implantation. But, the longest tumor diameters measured on arterial phase were 7.1 ± 3.2 cm at day 17 and 9.1 ± 5.9 cm at day 24, whereas the sizes were 6.2 ± 3.3 cm at day 17 and 8.3 ± 5.6 cm at day 24 on portal phase.

Group II (solitary tumor model): Twenty one rabbits out of 24 (87.5%) showed solitary tumor growth. A solitary nodule was observed on the left lobe during the entire follow-up period (Fig. 2). At day 10 post-implantation, hypoattenuating lesions with thick rim enhancement were detected on arterial phase (Fig. 2A), and the peripheral rim enhancement disappeared on portal phase (Fig. 2B). As time passed, the tumor sizes were increased without changes in enhancement patterns on day 17 (Fig. 2C, D) and 24 (Fig. 2E, F). An arterioportal shunt adjacent to the tumor periphery was obviously noticed on arterial phase at day 17 (arrow). The longest tumor diameters measured on arterial phase were 7.4 ± 0.7 cm, 14.2 ± 6.0 cm, and 17.4 ± 4.3 cm on day 10, 17 and 24, respectively. On the portal phase, the sizes were 5.7 ± 2.7 cm, 12.8 ± 5.2 cm and 16.1 ± 4.2 cm on day 10, 17 and 24, respectively.

Pathologic findings: Gross pathologic photographs of the liver are demonstrated for both groups (Fig. 3). In group I, viable tumor cells were mainly found at the fibrovascular core structure in the tumor center, and multiple thin walled cystic spaces were observed along the peripheral area (Fig. 4). This finding is compatible with the target appearance shown in the enhanced CT images. Little necrosis was observed in this group. In group II, the viable tumor cells of the solitary tumor were found in the periphery of the nodule, and central necrosis was apparent on day 24 after tumor implantation (Fig. 5). This finding is consistent with the peripheral rim enhancement and central hypointensity.

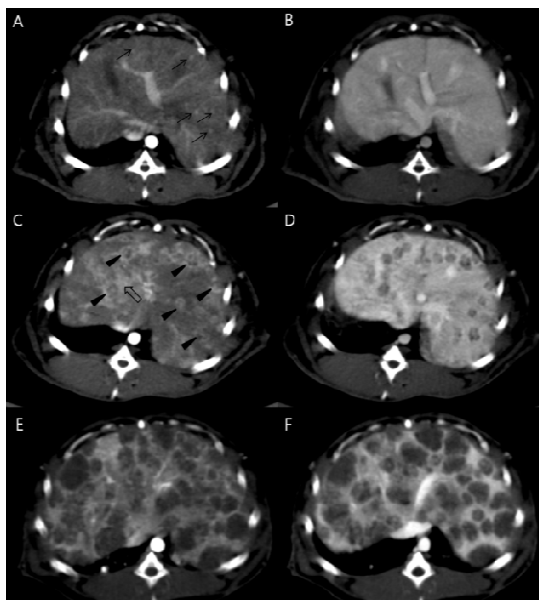


Fig. 1: Transverse CT images of multinodular disseminated VX2 tumors after tumor injection into a mesenteric vein (group I). At day 10 post implantation, arterial phase CT image (A) shows tiny enhancing lesions (arrows), which are not clearly observed on portal phase (B). On day 17, lesions are larger and show target appearances with central hyperdensity (arrowheads) on arterial (C) and portal (D) phases. At day 24, arterial (E) and portal (F) phases reveals more obvious target appearances of the lesions.

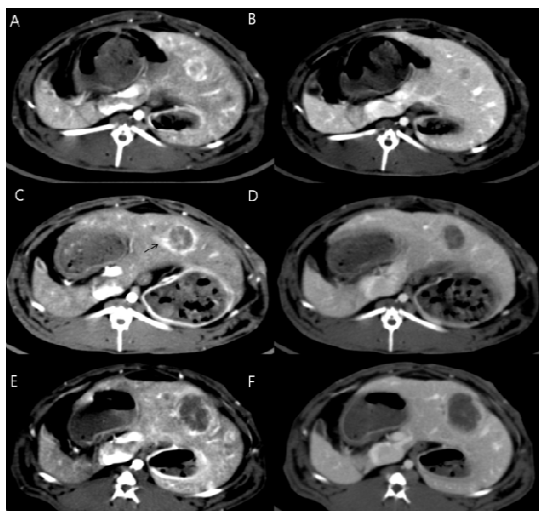


Fig. 2: Transverse CT images of solitary VX2 carcinoma after direct tumor inoculation onto the hepatic parenchyma (group II). At day 10 post implantation, arterial phase (A) shows hypodense lesion with thick peripheral enhancement, which disappears on portal phase (B). From day 17 (C,D) through day 24 (E,F), tumor becomes larger with the same enhancing pattern. C and E are arterial phase, whereas D and F are portal phase. An arterioportal shunt is demonstrated at day 17 (arrow).

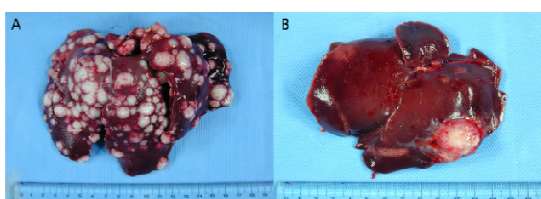


Fig. 3: Gross photograph of the liver harvested at day 24, A) group I, and B) group II.

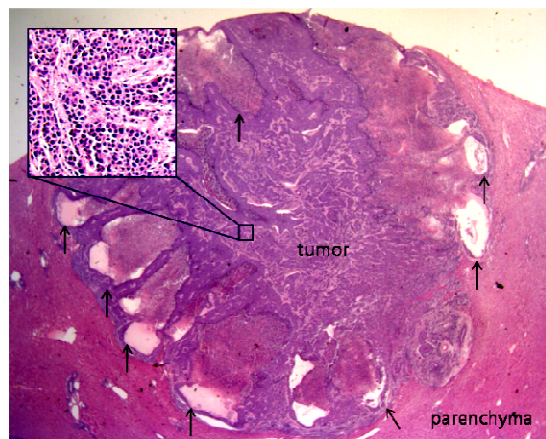


Fig. 4: Histopathological findings ($\times 12.5$) of hepatic VX2 tumors in group I. Tumors are surrounded by multiple, thin-walled sinusoidal vascular spaces (arrows). Viable tumor cells were mainly found at the fibrovascular core structure in the tumor center (magnified image at the left-upper corner, $\times 100$).

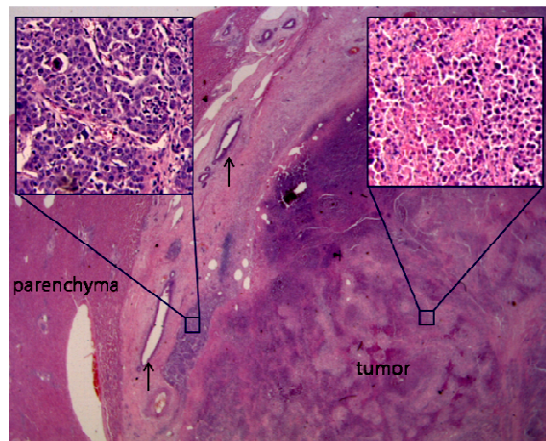


Fig. 5: Histopathological findings ($\times 12.5$) of hepatic VX2 tumors in group II. Solitary tumor with central necrosis is observed in the tumor center, whereas viable tumor cells are mainly located in the tumor periphery. Dilated vessels are observed along the tumor capsule (arrows).

DISCUSSION

The liver is an organ in which metastatic tumors usually take place as well as primary tumors. Metastatic tumor cells can invade the vascular space and migrate to the liver via the portal or arterial system. The VX2 carcinoma is a well-established cell for inducing hepatic tumors in radiologic and therapeutic studies (Schneider *et al.*, 1997; Lee *et al.*, 2008; Luo *et al.*, 2010; Sonoda *et al.*, 2012), and a metastatic model has been created by intraportal injection of VX2 carcinoma tumor cells in rabbits (Koishi *et al.*, 1994; Tanaka *et al.*, 1995; Kuwata *et al.*, 1997; Kapanen *et al.*, 2003). In our study, we created metastatic hepatic tumor model by injecting the tumor into the mesenteric vein rather than injecting directly into the portal vein, because the mesenteric vein is largely included in the portal system and directly connected to the main portal vein. Furthermore, as the portal vein is deep-seated behind the stomach and omentum, it is difficult to gain access to the portal vein during the laparotomy. On the other hand, the mesenteric vein is located superficially along the mesentery, and easily cannulated for injection of tumor suspension.

VX2 carcinomas show age-related changes in vascularity (Wu *et al.*, 2009), and are used in many studies for contrast medias, such as their nature, optimal concentration for systemic injection, and best timing of image acquisition (Leander, 1996; Weichert *et al.*, 2000). Conventional CT findings of hepatic VX2 carcinoma have been described in the previous reports (Lee *et al.*, 1997), but studies to examine CT characteristics of the tumors experimentally created by different methods (intraportal vs intraparenchymal induction) are not common. In this study, Solitary VX2 hepatoma created by direct tumor injection onto liver surface is hypointense in CT scan, which was same as in previous reports (Jia *et al.*, 2000). Additionally we noticed the thick rim enhancing area in arterial phase disappeared in portal phase. Though most metastatic tumors created by mesenteric vein injection showed similar hypointensity, the 'hyperattenuating central area' made the metastatic tumors look different from the solitary tumor.

Interestingly, these unique CT characteristics of metastatic and solitary hepatic tumor models are compatible with histopathological examination. Group I showed a target shape on both the arterial and portal phases of CT scans. Although the reason for this imaging pattern is unclear, several suggestions for this observation can be made from the histopathologic features. The tumors had a fibrovascular structure in the central core, and peripherally located cystic spaces. We can assume that 'target sign' on CT can occur from blood vessel-containing core structures, which also provides resistance to ischemic necrosis of the lining tumor cells. We found little necrosis of the nodules in this metastatic model until the end of the follow-up period. We found the arterioportal shunts reported previously in an intraportal injection model (Lee *et al.*, 2008), and in a direct inoculation model as well.

For intraparenchymal inoculation, a fragment of tumor tissue has been implanted instead of a cell suspension. Transplantation of a tumor fragment limit tumor growth to a localized area, and there is no risk of initial spread or leakage of the tumor tissue (Phillips *et al.*, 1992; Thorstensen *et al.*, 1994). Here, in group II, the solitary tumor showed general enhancement on day 10 after tumor implantation, and peripheral enhancement with central hypodensity later, consistent with previous work (Iyer and Charnsangavej, 1998). The age-dependent central hypodensity indicates poor central vascularity that induced necrosis in the enlarged solitary tumor.

Since hepatic tumor is a common challenge in oncologic studies, the establishment and comprehensive understandings of the tumor models are essential for the preclinical research of the diseases. To the author's knowledge, no report compared the sequential CT imaging characteristics between metastatic and solitary hepatic tumor model established by different methods.

Conclusion: A metastatic hepatic tumor induced in the rabbit liver has a characteristic target appearance on CT scans, which is different from the solitary hepatic tumor. Differences in imaging may be useful for radiological analysis of therapeutic responses using the rabbit VX2 carcinoma model. Though this report could not provide direct information of human hepatic tumor, it can benefit future studies of novel diagnostic or therapeutic strategies.

REFERENCES

- Gnant MR, LA Noll, KR Irvine, M Puhlmann, RE Terrill, HR Jr Alexander and DL Bartlett, 1999. Tumor-specific gene delivery using recombinant vaccinia virus in a rabbit model of liver metastases. *J Natl Cancer Inst*, 20: 1744-1750.
- Iyer R and C Charnsangavej, 1998. Imaging Studies for Hepatobiliary Tumors. In: Liver cancer (Curley SA, eds), Springer, New York, USA, pp: 1-25.
- Jia HS, XY Quan, S Zeng and ZB Wen, 2002. Dynamic evaluation of rabbit VX2 hepatic carcinoma with CT and MRI. *Di Yi Jun Yi Da Xue Xue Bao*, 22: 141-144.
- Kapanen MK, JT Halavaara and AM Häkkinen, 2003. Assessment of vascular physiology of tumorous livers: comparison of two different methods. *Acad Radiol*, 10: 1021-1029.
- Koishi Y, H Taniguchi, H Tanaka, T Higashida, K Takeuchi, K Miyata, H Koyama, M Masuyama and T Takahashi, 1994. Inhibition of liver metastases in rabbits by arterial infusion of angiogenesis inhibitor, TNP-470. *Gan To Kagaku Ryoho*, 21: 2118-2120.
- Kuwata Y, S Hirota and M Sako, 1997. Treatment of metastatic liver tumors by intermittent repetitive injection of an angiogenesis inhibitor using an implantable port system in a rabbit model. *Kobe J Med Sci*, 43: 83-98.
- Leander P, 1996. A new liposomal contrast medium for CT of the liver. An imaging study in a rabbit tumour model. *Acta Radiol*, 37: 63-68.
- Lee FT, SG Chosy, SG Naidoo, S Goldfarb, JP Weichert, DA Bakan, JE Kuhlman, RH Tambeaux and IA Sproat, 1997. CT depiction of experimental liver tumors: contrast enhancement with hepatocyte-selective iodinated triglyceride versus conventional techniques. *Radiology*, 203: 465-470.
- Lee KH, E Liapi, M Buijs, JA Vossen, V Prieto-Ventura, LH Syed and JF Geschwind, 2008. Percutaneous US-guided implantation of Vx-2 carcinoma into rabbit liver: a comparison with open surgical method. *J Surg Res*, 155: 94-99.
- Luo W, X Zhou, X Zheng, G He, M Yu, Q Li and Q Liu, 2010. Role of sonography for implantation and sequential evaluation of a VX2 rabbit liver tumor model. *J Ultrasound Med*, 29: 51-60.
- Phillips PC, TT Than, LC Cork, J Hilton, BS Carson, OM Colvin and LB Grochow, 1992. Intrathecal 4-hydroperoxycyclophosphamide: neurotoxicity, cerebrospinal fluid pharmacokinetics, and antitumor activity in a rabbit model of VX2 leptomeningeal carcinomatosis. *Cancer Res*, 52: 6168-6174.
- Schneider M, A Broillet, P Bussat, N Giessinger, J Puginier, R Ventrone and F Yan, 1997. Gray-scale liver enhancement in VX2 tumor-bearing rabbits using BR14, a new ultrasonographic contrast agent. *Invest Radiol*, 32: 410-417.
- Seo TS, JH Oh, DH Lee, YT Ko and Y Yoon, 2001. Radiologic anatomy of the rabbit liver on hepatic venography, arteriography, portography, and cholangiography. *Invest Radiol*, 36: 186-192.
- Shope RE and EW Hurst, 1993. Infectious papillomatosis of rabbits: With a note on the histopathology. *J Exp Med*, 58: 607-624.
- Sonoda A, N Nitta, A Nitta-Seko, S Ohta, Y Nagatani, K Mukaiho, H Otani, K Tsuchiya, M Takahashi and K Murata, 2011. Time-course studies of implanted rabbit VX2 liver tumors to identify the appropriate time for starting hepatic arterial embolization in animal models. *Oncology*, 80: 92-96.
- Tanaka H, H Taniguchi, T Mugitani, Y Koishi, M Masuyama, T Higashida, H Koyama, Y Suganuma, K Miyata, K Takeuchi and T Takahashi, 1995. Intra-arterial administration of the angiogenesis inhibitor TNP-470 blocks liver metastasis in a rabbit model. *Br J Cancer*, 72: 650-653.
- Thorstensen O, B Isberg, U Svahn, H Jorulf, N Venizelos and G Jarekko, 1994. Experimental tissue transplantation using a biopsy instrument and radiologic methods. *Invest Radiol*, 29: 469-471.
- Weichert JP, FT Jr Lee, SG Chosy, MA Longino, JE Kuhlman, DM Heisey and GE Leverson, 2000. Combined hepatocyte-selective and blood-pool contrast agents for the CT detection of experimental liver tumors in rabbits. *Radiology*, 216: 865-871.
- Wolf CW, CA Presant, KL Servis, A el-Tahtawy, MJ Albright, PB Barker, R Ring, D Atkinson, R Ong, M King, M Singh, M Ray, C Wiseman, D Blayne and J Shani, 1990. Tumor trapping of 5-fluorouracil: in vivo ¹⁹F NMR spectroscopic pharmacokinetics in tumor-bearing humans and rabbits. *Proc Natl Acad Sci USA*, 87: 492-496.
- Wu H, AA Exner, H Shi, J Bear and JR Haaga, 2009. Dynamic evolutionary changes in blood flow measured by MDCT in a hepatic VX2 tumor implant over an extended 28-day growth period: time-density curve analysis. *Acad Radiol*, 16: 1483-1492.